Supporting Information

For

Expanded Rosarin. A Versatile Fullerene (C_{60}) Receptor

Xian-Sheng Ke[†], Taeyeon Kim[‡], James T. Brewster II[†], Vincent M. Lynch[†], Dongho Kim[*‡], and Jonathan L. Sessler[*†]

[†] Department of Chemistry, The University of Texas at Austin, Austin, Texas 78712-1224, United States.

[‡] Department of Chemistry, Yonsei University, Seoul 120-749, Korea

Email: sessler@cm.utexas.edu; dongho@yonsei.ac.kr

Table of Contents

1. **General information**
2. **Synthesis and characterization**
3. **^{1}H NMR spectroscopic titrations**
4. **UV and fs-TA spectral studies**
5. **Supporting crystal data and X-ray experimental details**
6. **DFT calculation details**
7. **References**

1. General information

All solvents and chemicals used were purchased from Aldrich, TCI, or Acros and used without further purification. TLC analyses were carried out using Sorbent Technologies silica gel (200 mm) sheets. Column chromatography was performed on Sorbent silica gel 60 (40–63 mm). NMR spectra were recorded on a Varian Mercury 400 instrument. The NMR spectra were referenced to solvent residue peaks and the spectroscopic solvents were purchased from Cambridge Isotope Laboratories and Aldrich). High resolution ESI mass spectra were taken on an Ion Spec Fourier Transform mass spectrometer (9.4 T). UV-vis spectra were measured on a Varian Cary 5000 spectrophotometer. Electrospray ionization (ESI) mass spectra were recorded on Waters Micromass AutoSpec Ultima and Agilent Technologies 6530 Accurate-Mass Q-TOF instruments. X-ray crystallographic analyses were carried out on an Agilent Technologies SuperNova Dual Source diffractometer using a μ-focus Cu Kα radiation source (λ = 1.5418 Å) with collimating mirror monochromators.

2 Synthesis and characterization

To 2,6-bis(3,4-diethyl-2-pyrryl) pyridine (644 mg, 2 mmol) were added propionic acid (300 ml) and benzaldehyde (0.7 mL, 3.5 equiv, 7 mmol). The reaction mixture was purged with nitrogen and then stirred for 20 h at 125º. After allowing the mixture to cool down to room temperature, propionic acid was removed by evaporation. The resulting residue was redissolved by dichloromethane (200 mL) and 2,3-dichloro-5,6-dicyanoquinone (DDQ) (1.1 g, 5 mmol) was then added. The reaction mixture was stirred for 2 h at room temperature. The reaction mixture was then transferred to a neutral alumina column and eluted with CH_2Cl_2/acetone (v/v = 10:1-5:1). After removing the organic solvent, the residue was recrystallized from CH_2Cl_2-hexanes to give a red powder. Yield: 120 mg, 15%. ^{1}H NMR (400 MHz, $CDCl_3$) δ 13.00 (s, 3H), 7.72(m, 6H), 7.65 (m, 3H), 7.43(m, 9H), 7.35(m, 6H), 2.75 (q, J = 7.4 Hz, 12H), 1.80 (q, J = 7.4 Hz, 12H), 1.04 (t, J = 7.4 Hz, 18H), 0.76 (t, J = 7.4 Hz, 18H). ^{13}C NMR (101 MHz, $CDCl_3$) δ 153.0, 150.7, 142.01, 139.98, 138.6, 137.8, 136.8, 133.5, 130.1, 128.6, 120.9, 18.5, 18.1, 16.6, 15.4. UV/Vis (CH_2Cl_2): λ_{max} (ε M^{-1} cm^{-1}) = 303 (73,734) and 487 (67,772). HRMS (ESI^+) *m/z* $[M + 2H]^{2+}$: calcd for $C_{84}H_{87}N_9$ 611.8615, found: 611.8620.

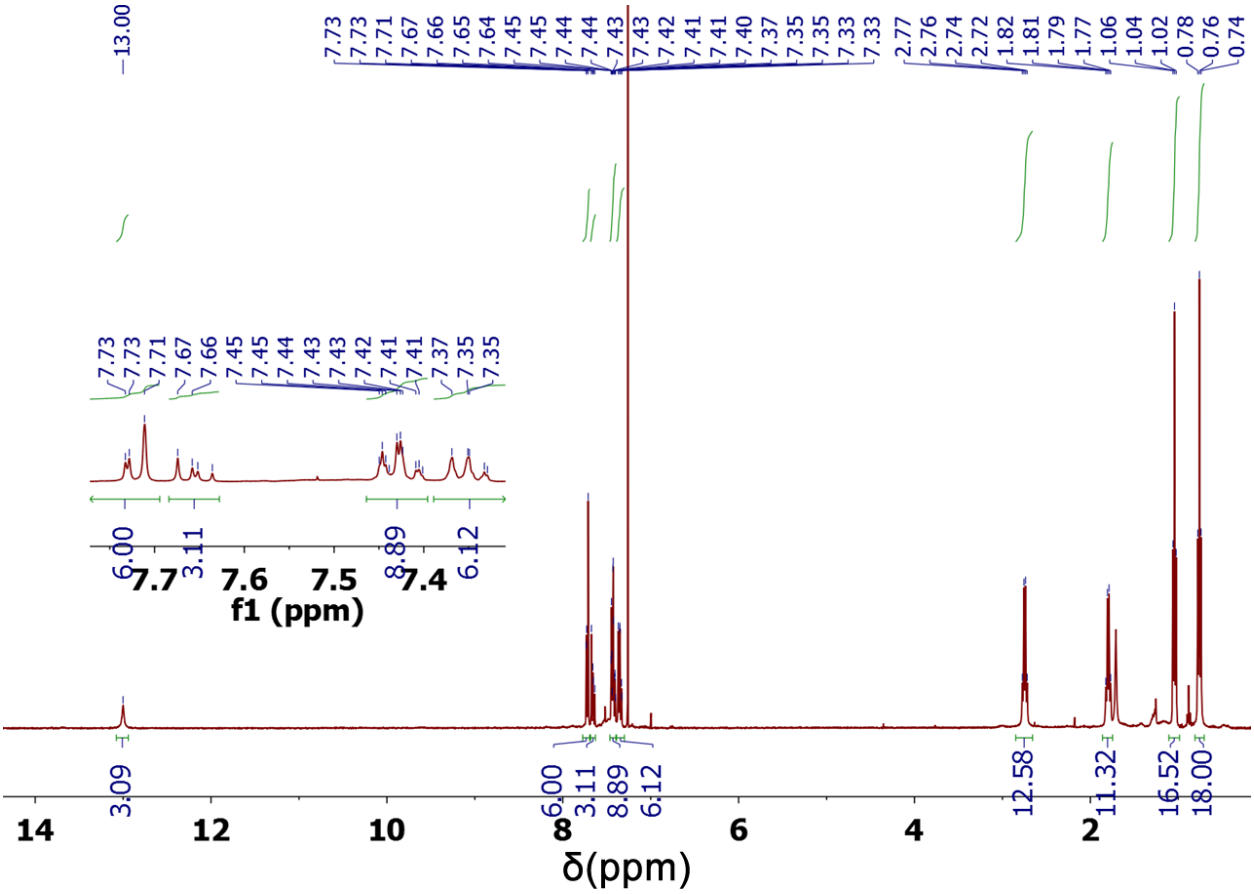

Figure S1. ^{1}H NMR spectrum of $\mathbf{P_3P_6}$ in $CDCl_3$.

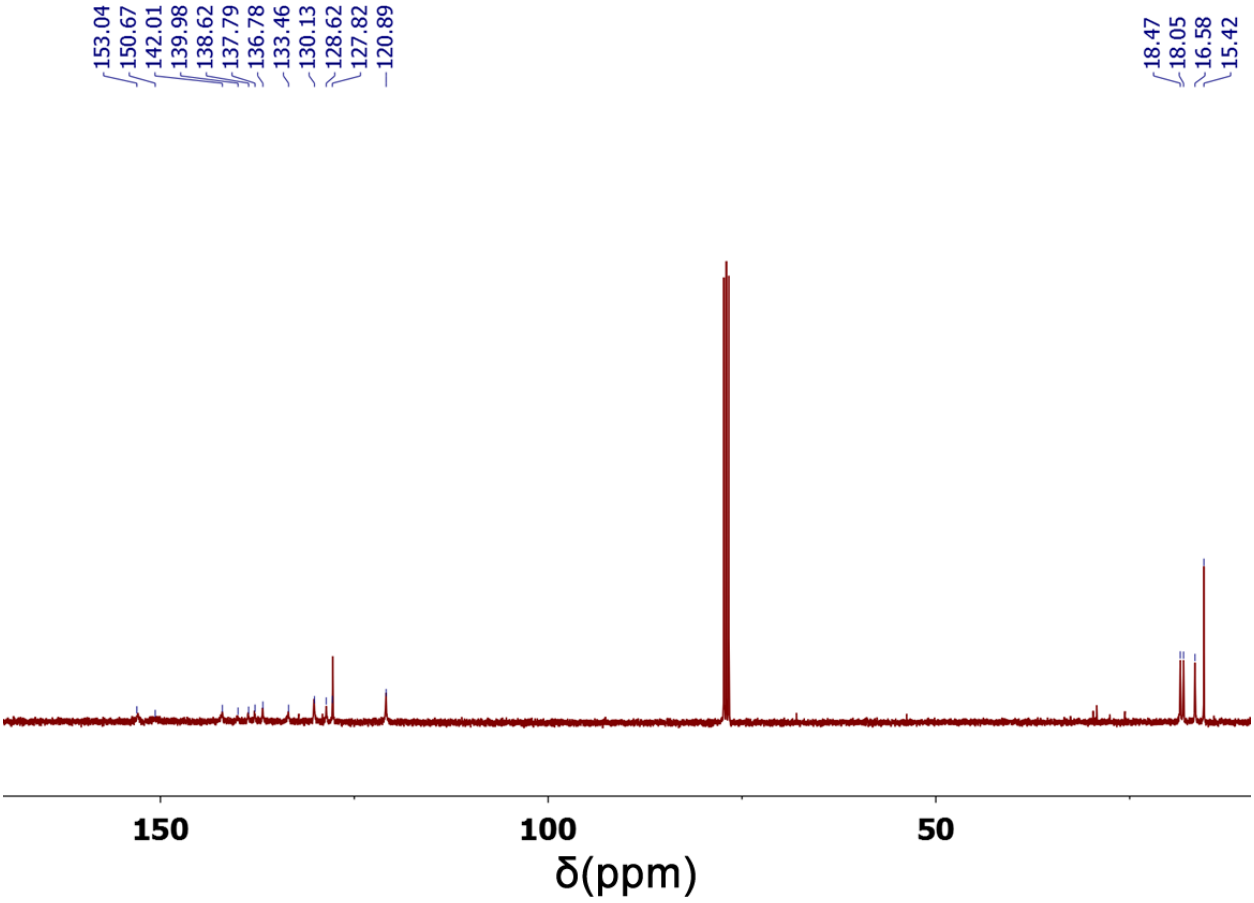

Figure S2. ^{13}C NMR spectrum of $\mathbf{P_3P_6}$ in $CDCl_3$.

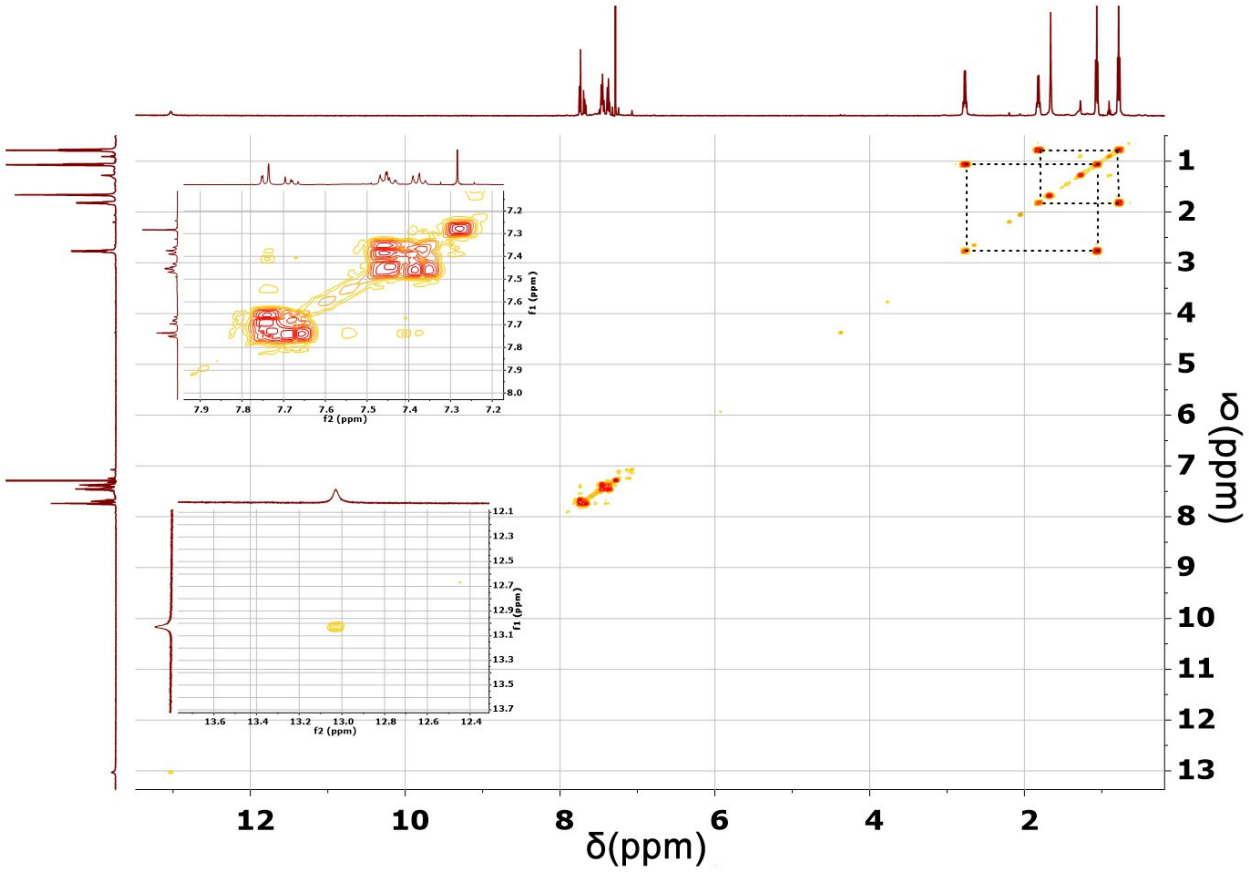

Figure S3. ^{1}H-^{1}H COSY spectrum of $\mathbf{P_3P_6}$ in $CDCl_3$.

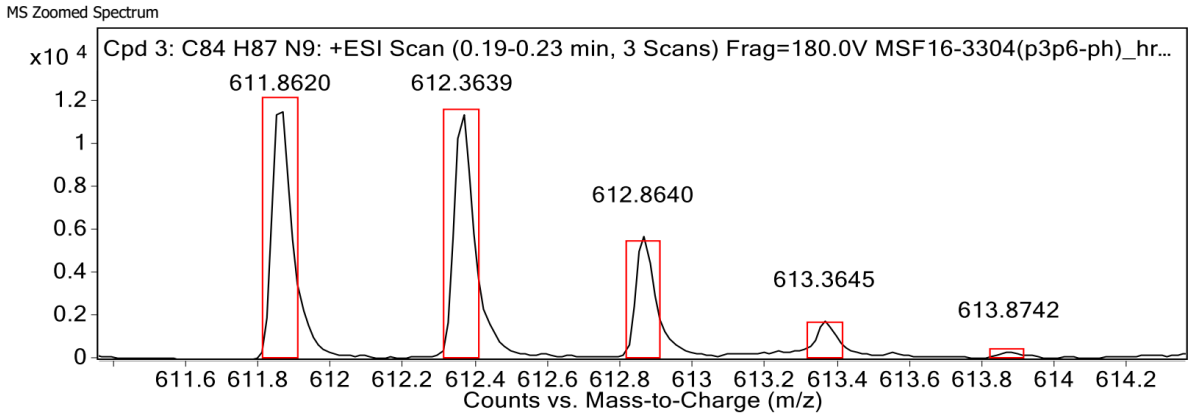

MS Spectrum Peak List

Obs. m/z	Calc. m/z	Charge	Abund	Formula	Ion/Isotope	Tgt Mass Error (ppm)
360.32480			13672.66			
611.86200	611.86150	2	11835.66	C84H87N9	(M+2H)+2	-0.89
612.36390	612.36310	2	11453.7	C84H87N9	(M+2H)+2	-1.29
612.86400	612.86470	2	5741.74	C84H87N9	(M+2H)+2	1.07
613.36450	613.36620	2	1795.68	C84H87N9	(M+2H)+2	2.83
613.87420	613.86780	2	371.89	C84H87N9	(M+2H)+2	-10.46

Figure S4. HR-ESI mass spectrum of $\mathbf{P_3P_6}$.

3. ^{1}H NMR spectroscopic titrations

A stock solution of $\mathbf{P_3P_6}$ was prepared by dissolving 6.13 mg in 1.0 mL of deuterated 1,2-dichlorobenzene (ODCB-d_4) (to provide a starting solution of 5.00 x 10^{-3} M). 600 µL of the above solution was subsequently titrated with 20, 40, 60, 80, 100, 120, 140, 160, 180, 200, 250, 300, 400, 500, 700, 900, 1300 and 1700 µL of a 15.1 x 10^{-3}M solution of C_{60} in ODCB-d_4. The ^{1}H NMRspectra were recorded after each addition at ambient temperature. Significant chemical shift changes were observed for the inner NH ($\Delta\delta$ = 0.70 ppm) and pyridine β-H ($\Delta\delta$ = 0.14 ppm) protons. A stacked view of the resulting ^{1}H NMR spectra for these spectral regions is given in Figure S5 below. No obvious changes in the ^{1}H NMR chemical shifts of the $\mathbf{P_3P_6}$ resonances were seen upon dilution over the concentration ranges studied in ODCB-d_4 in the absence of C_{60}. Thus, it is concluded that host dimerization is negligible under conditions of the titration experiment.

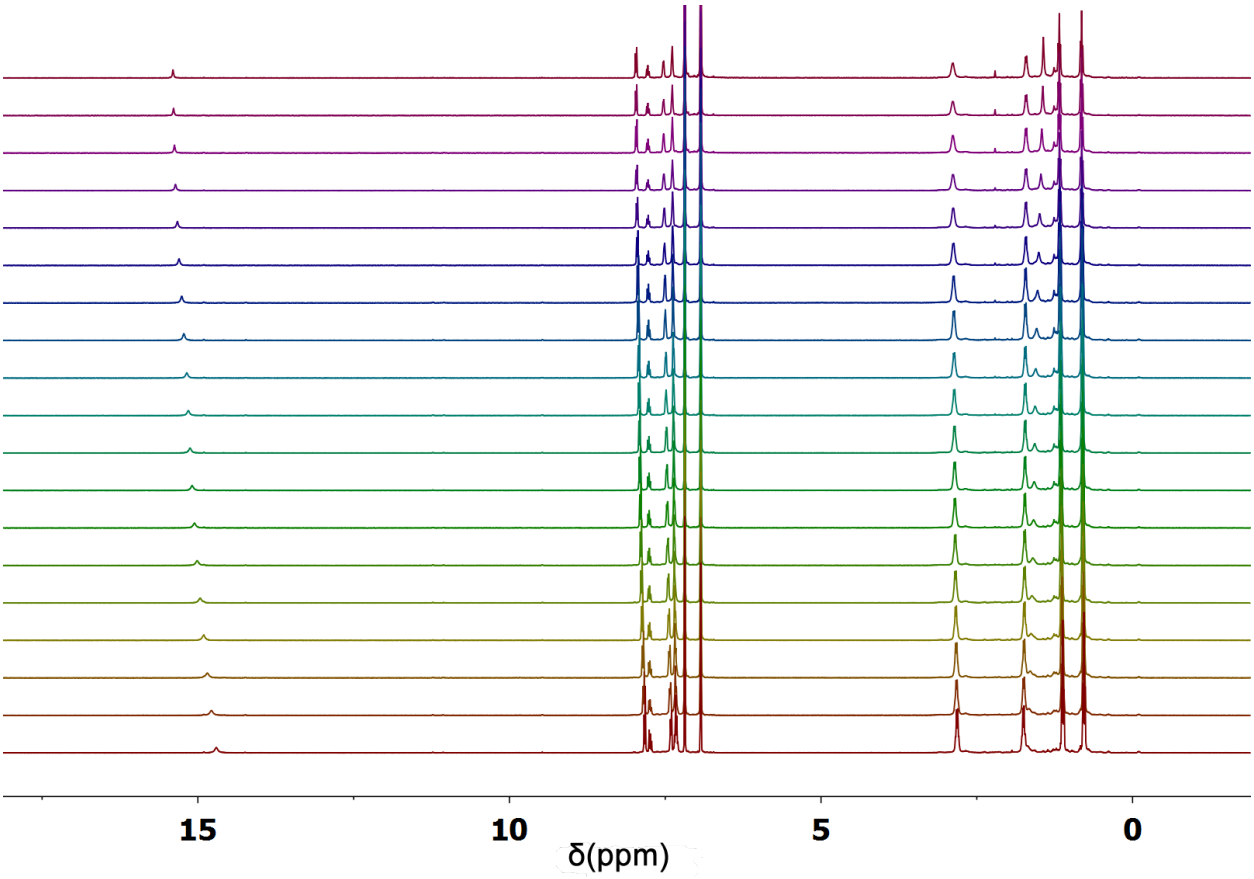

Figure S5. Proton NMR spectral titration of $\mathbf{P_3P_6}$ with C_{60} in ODCB-d_4.

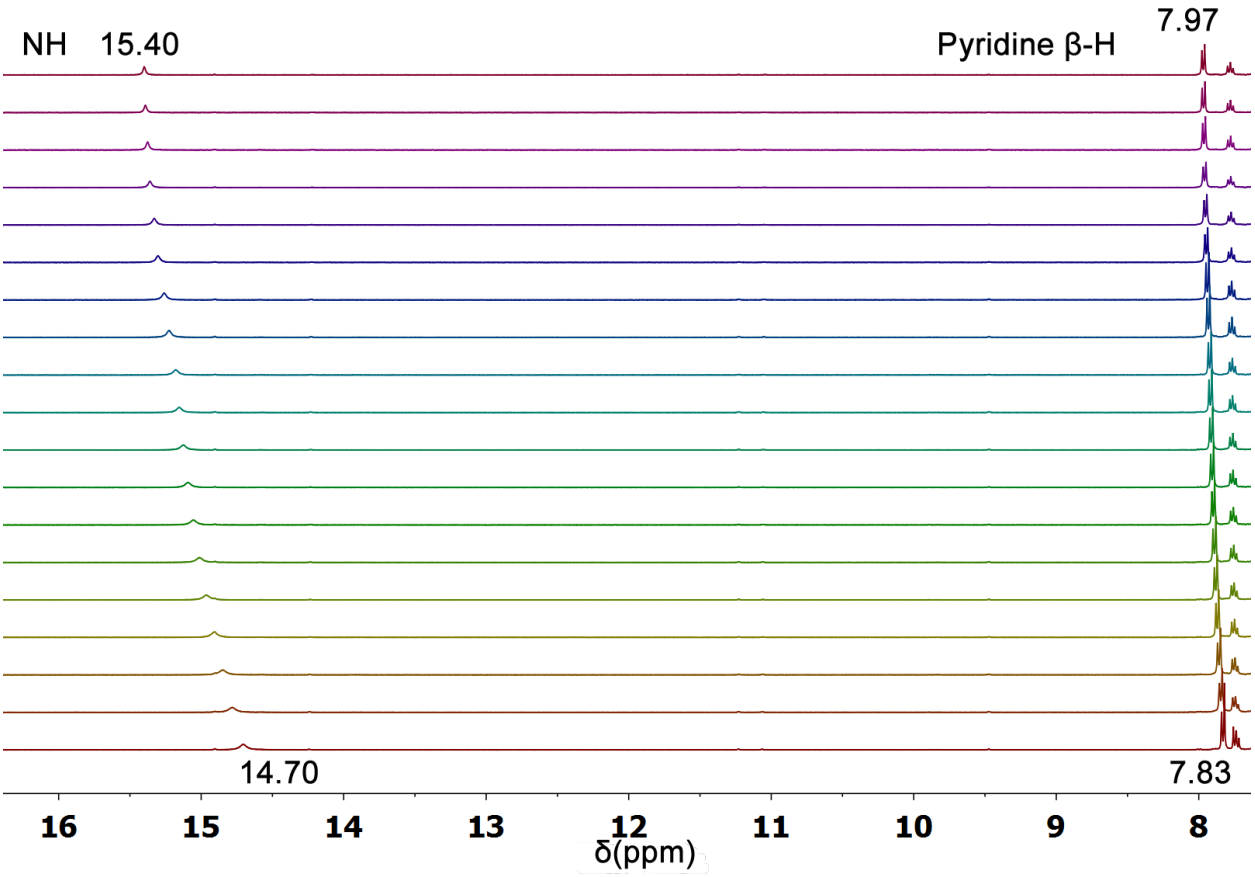

Figure S6. Partial proton NMR titration spectra of $\mathbf{P_3P_6}$ recorded upon adding C_{60} in ODCB-d_4.

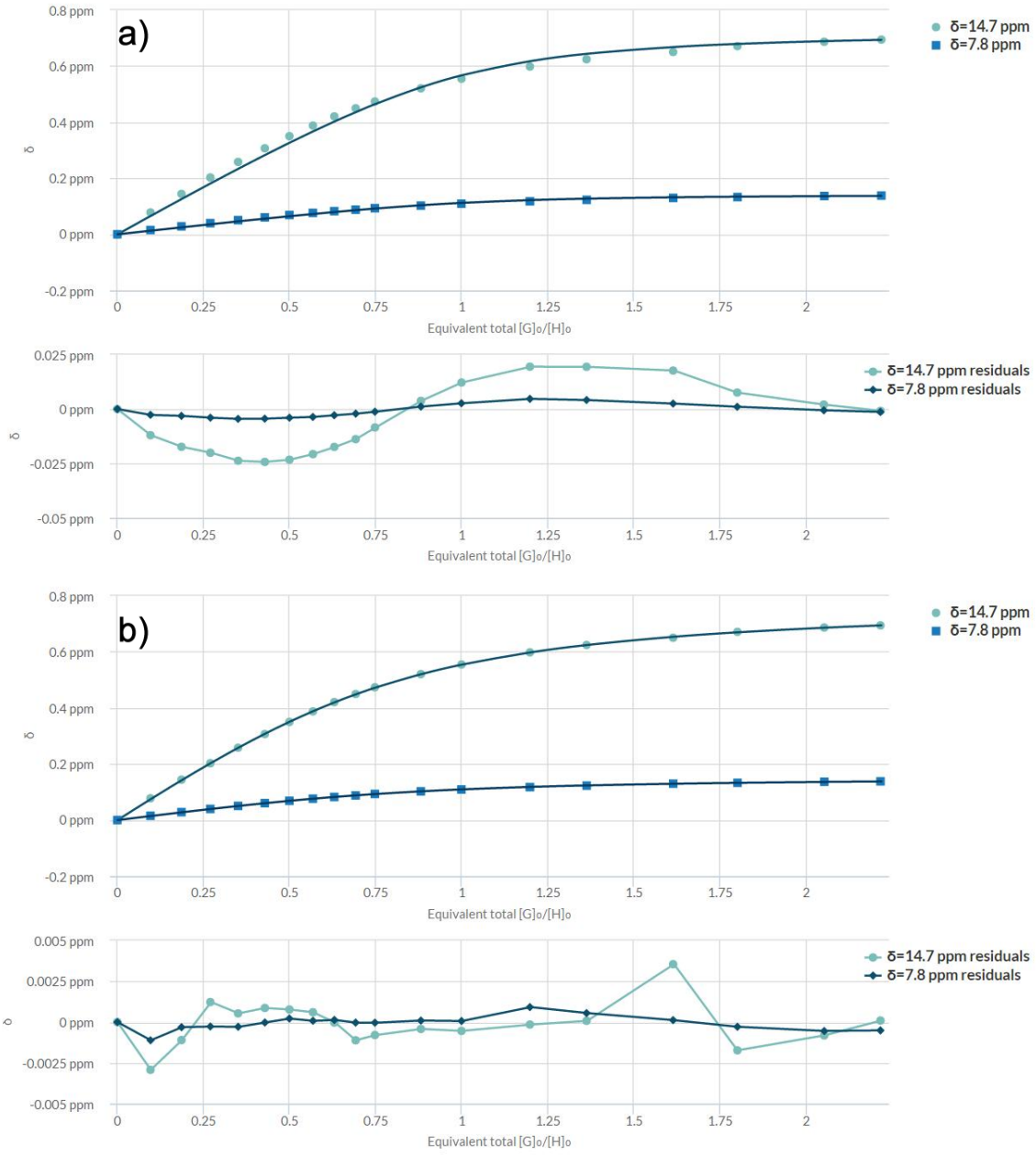

Figure S7. Fitting results obtained by using the a) 1:1 and b) 2:1 binding models associated with the program BindFit developed by P. Thordarson.[1]. K_a was evaluated from the changes of the chemical shifts of the two symmetry independent protons of the $\mathbf{P_3P_6}$ with obvious chemical shift changes. Based on a 1:1 binding model, the K_a value was calculated as 3195 ± 415 M^{-1} using this data set. Lower errors are seen if the data was fitted to a 2:1 (host: guest) model; this fitting gave K_{11} and K_{21} as 2209 ± 29 and 262 ± 11 M^{-1}, respectively.

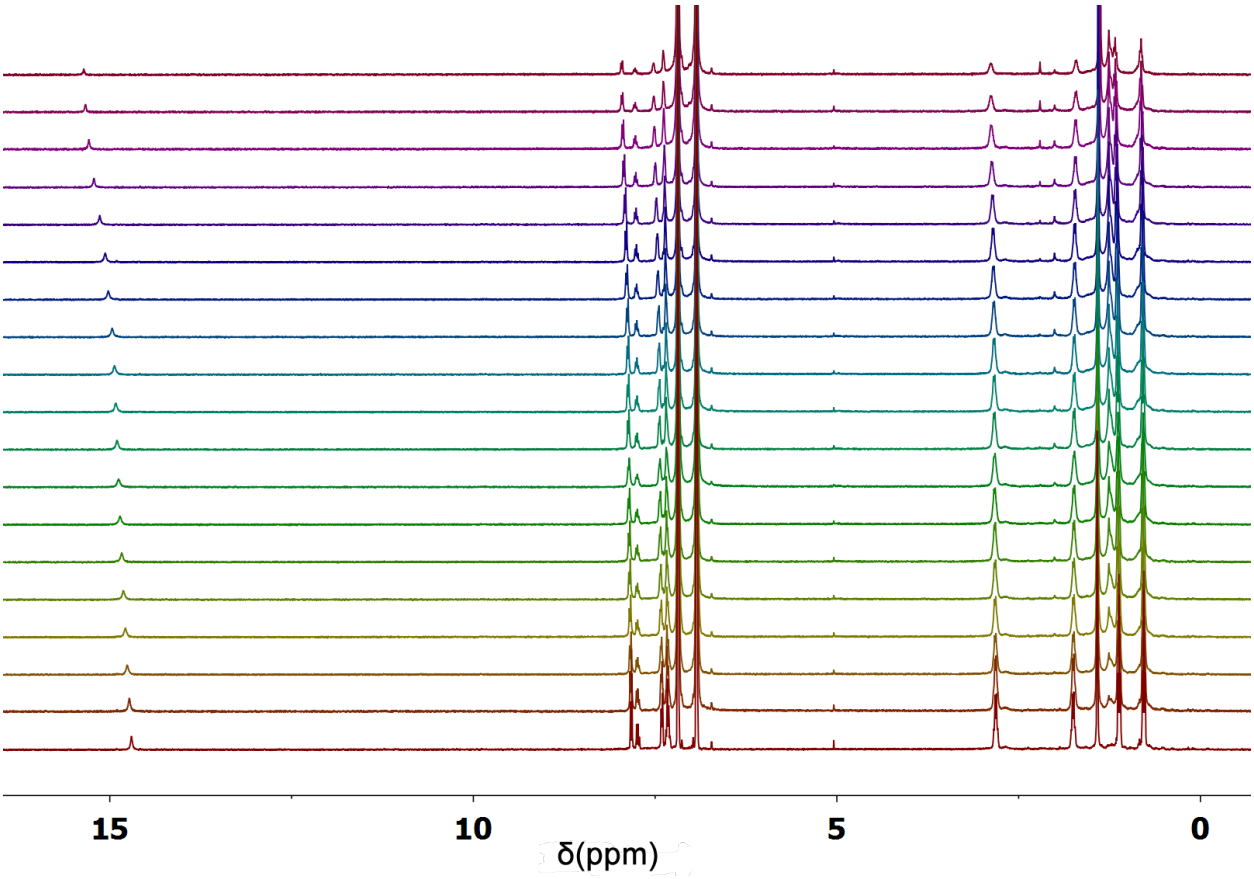

Figure S8. Proton NMR spectral titration of $\mathbf{P_3P_6}$ with C_{60} in ODCB-d_4 with a starting host concentration of 0.91 mM. This solution (600 µL) was then titrated with 5, 10, 15, 20, 25, 30, 35, 40, 45, 50, 60, 80, 100, 150, 250, 450, 850 and 1650 µL of a 9.96 mM solution of C_{60} in ODCB-d_4.

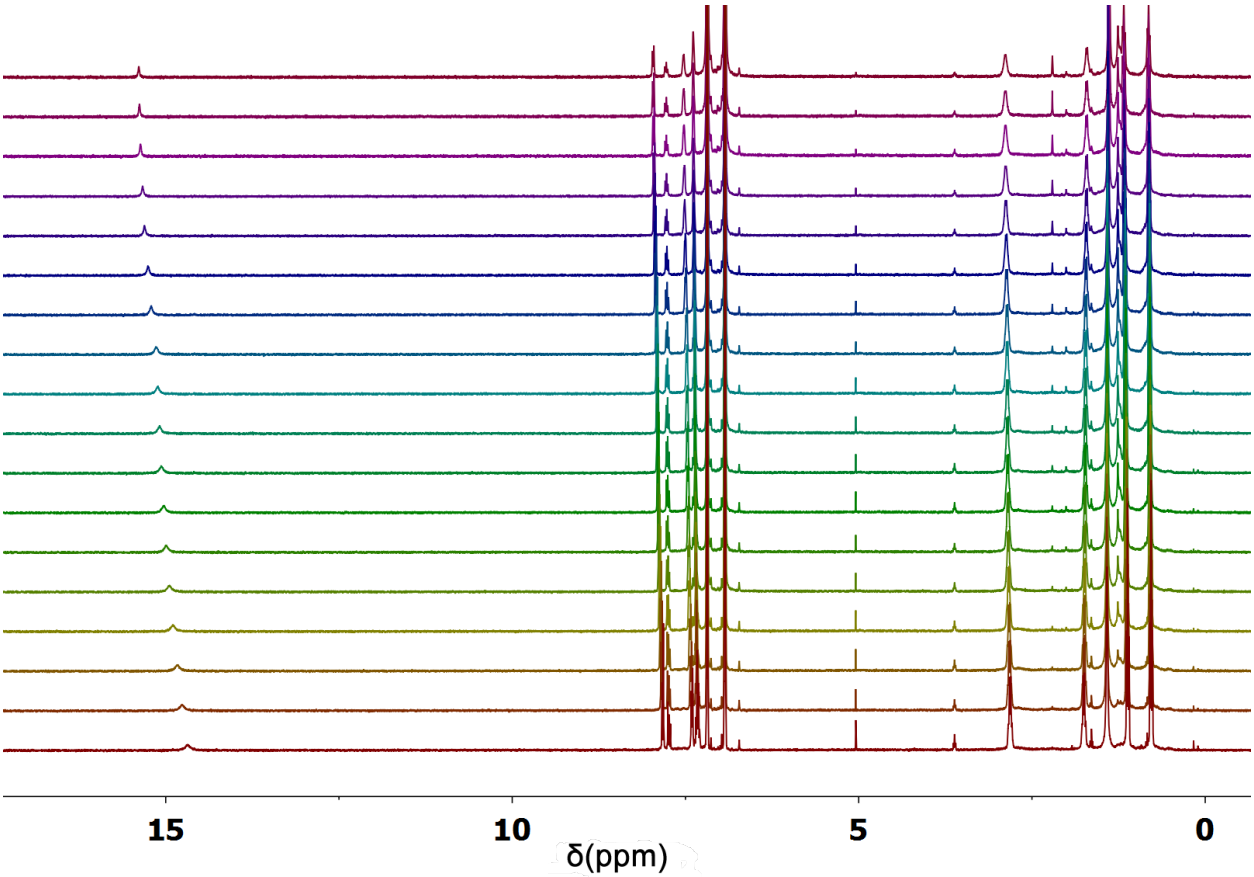

Figure S9. Proton NMR spectral titration of $\mathbf{P_3P_6}$ with C_{60} in ODCB-d_4 using a starting host concentration of 1.23 mM. This solution (600 µL) was then titrated with 10, 20, 30, 40, 50, 60, 70, 80, 90, 100, 150, 200, 300, 400, 600, 800 and 1000 µL of a 15.4 mM solution of C_{60} in ODCB-d_4.

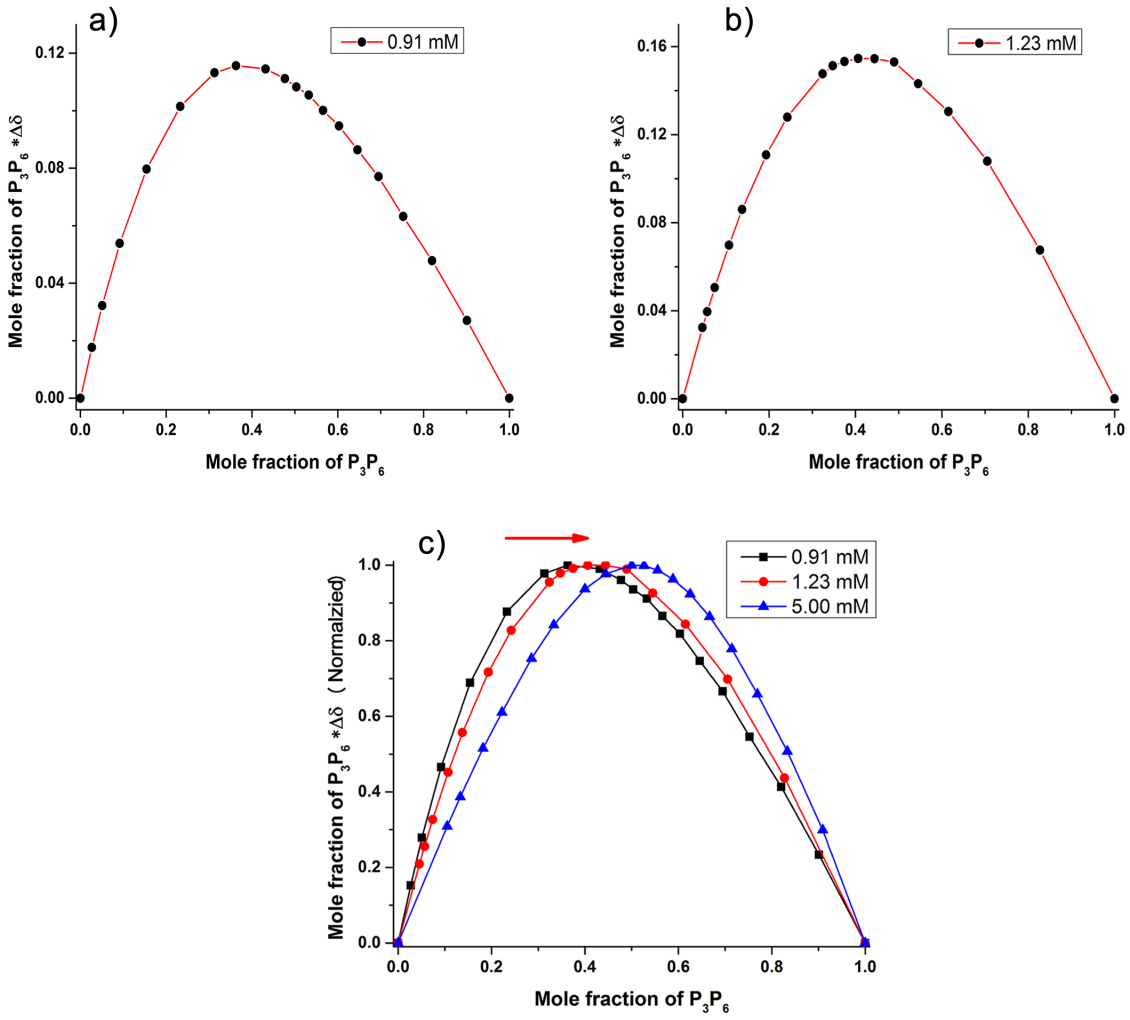

Figure S10. Job plots constructed from the chemical shift changes during ^{1}H NMR spectral titrations of **P_3P_6** with C_{60} in ODCB-d_4 where the starting concentration of **P_3P_6** was a) 0.91 and b) 1.23 mM, respectively. c) Comparison of normalized Job plots constructed from the chemical shift changes during ^{1}H NMR spectral titrations of **P_3P_6** with C_{60} in ODCB-d_4 where the starting concentration of **P_3P_6** was 0.91, 1.23, and 5.00 mM, respectively.

4. UV and fs-TA spectral studies

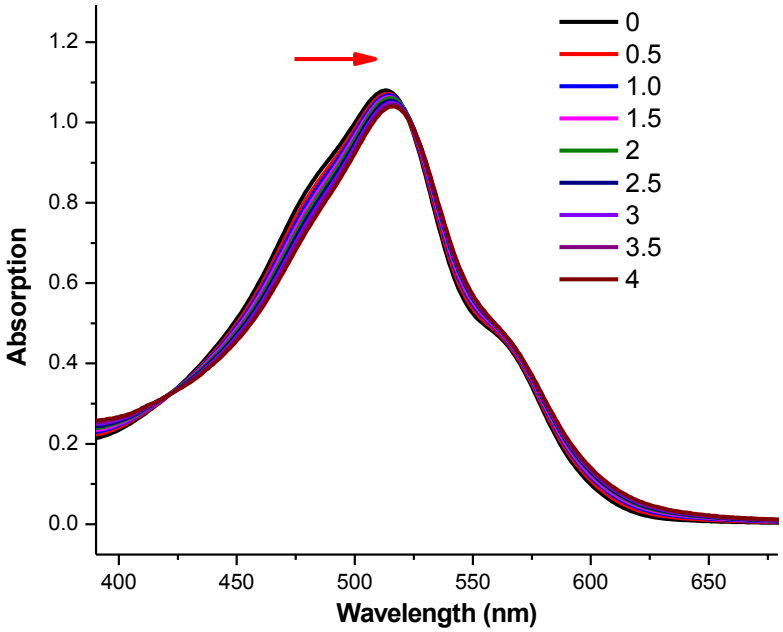

Figure S11. UV–vis spectra changes seen for $\mathbf{P_3P_6}$ upon adding different quantities of C_{60} in toluene.

Femtosecond Transient Absorption Measurements. The femtosecond time-resolved transient absorption (TA) spectrometer consisted of Palitra (optical parametric amplifier (OPA), S3 Quantronix) pumped by a Ti:sapphire regenerative amplifier system (Integra-C, Quantronix) operating at 1 kHz repetition rate and an optical detection system. The generated visible pulses by OPA had a pulse width of ~ 100 fs and an average power of 1 - 30 mW in the range 4_{60}-800 nm which were used as pump pulses. White light continuum (WLC) probe pulses were generated using a sapphire window (3 mm of thickness) by focusing of small portion of the fundamental 800 nm pulses which was picked off by a quartz plate before entering to the OPA. The time delay between pump and probe beams was carefully controlled by making the pump beam travel along a variable optical delay (ILS250, Newport). Intensities of the spectrally dispersed WLC probe pulses were monitored by miniature spectrograph (USB2000+, OceanOptics). To obtain the time-resolved transient absorption difference signal (ΔA) at a specific time, the pump pulses were chopped at 25 Hz and the absorption spectra intensities were saved alternately with or without the pump pulse. Typically, 6000 pulses were used excite samples to obtain the TA spectra at a particular delay time. The polarization angle between the pump and probe beams was set at the magic angle (54.7°) using a Glan-laser polarizer with a half-wave retarder in order to prevent polarization-dependent signals. The cross-correlation fwhm in the pump-probe experiments was less than 200 fs while the chirp of WLC probe pulses was measured to be 800 fs in the 400-800 nm region. To minimize chirp, all-reflection optics in probe beam path and 2 mm path length of quartz cell were used. After fluorescence and TA experiments, the absorption spectra of the sample was checked to avoid artifacts from degradation and photo-oxidation of samples. HPLC grade solvents were used in all steady-state and time-resolved spectroscopic studies.

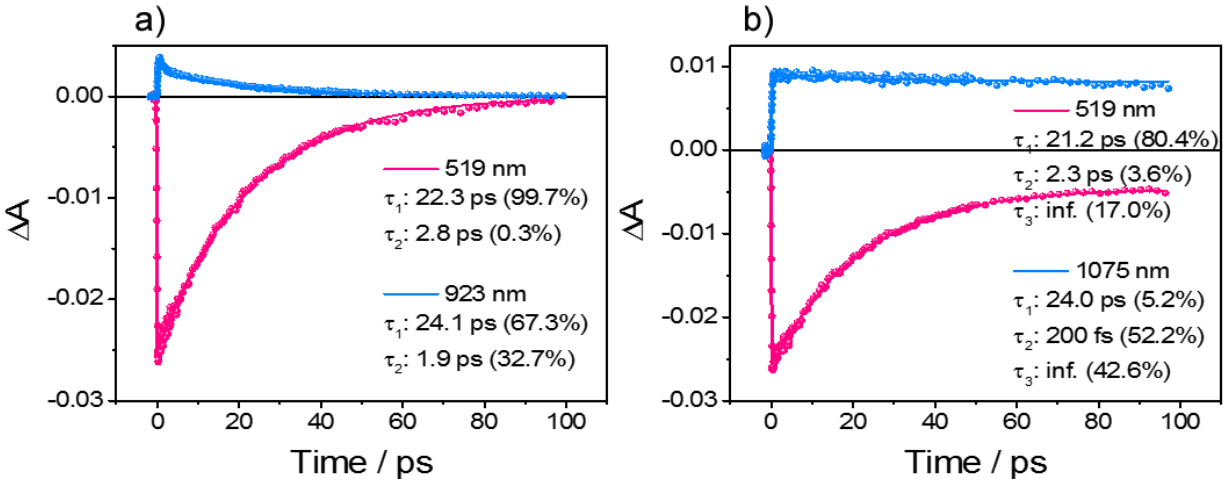

Figure S12. Kinetic traces with fitted lines associated with the ground state bleaching (GSB) and excited state absorption (ESA) of a) $\mathbf{P_3P_6}$ only and b) $\mathbf{P_3P_6}$ with 1 equiv. C_{60}. A pump wavelength of 500 nm was used. Measurements were made over the visible and NIR region (up to 1200 nm) spectral regions.

5. Supporting crystal data and X-ray experimental details

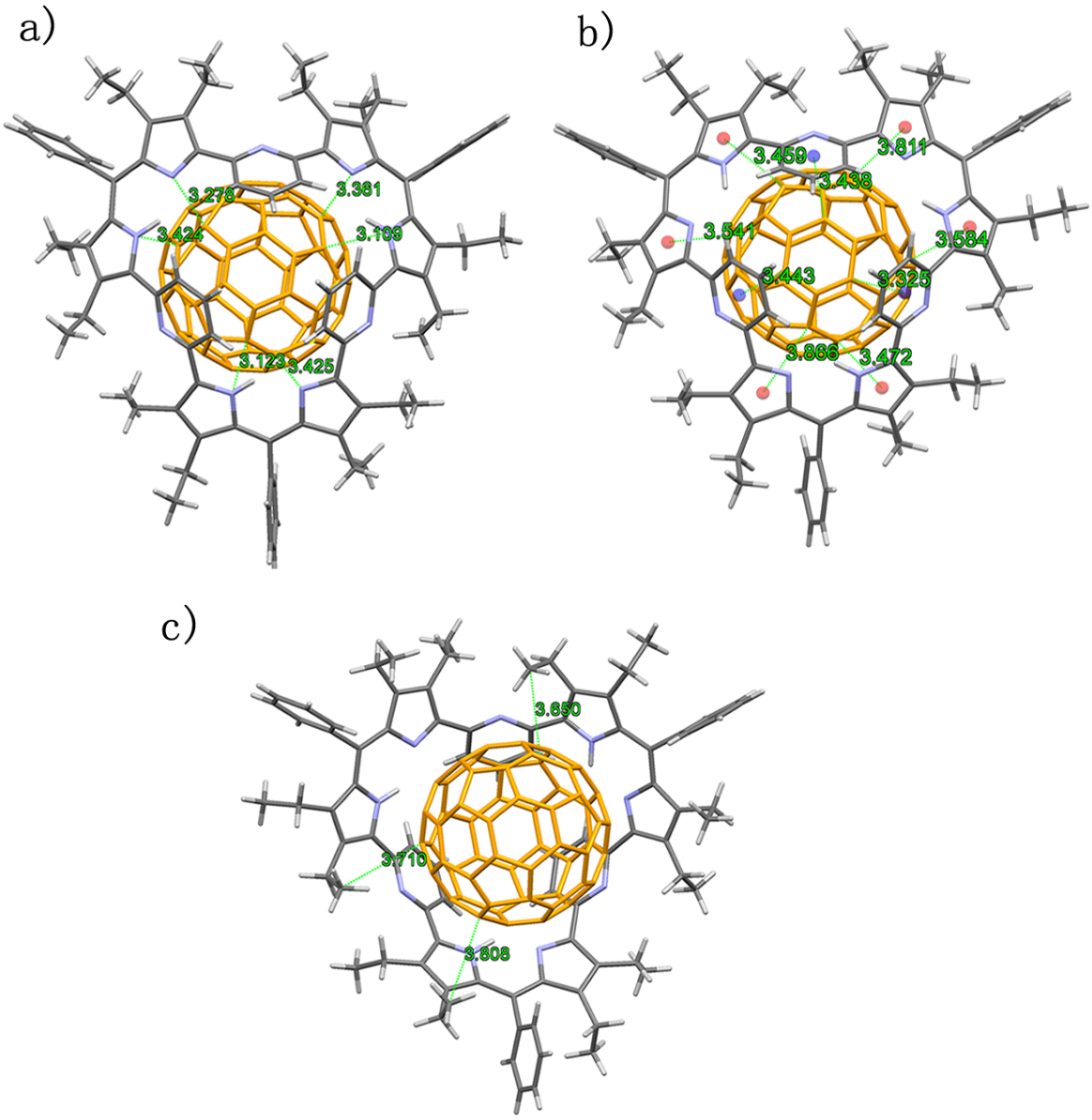

Figure S13. Interactions between $\mathbf{P_3P_6}$ and C_{60} seen in the $\mathbf{P_3P_6}$•C_{60} 1:1 complex. a) distances (Å) between the pyrrolic N and C_{60}; b) distances (Å) of the centroids of the pyrrole (red ball) and pyridine (blue ball) rings to C_{60}; c) selective distances from the alkyl substituents to C_{60}.

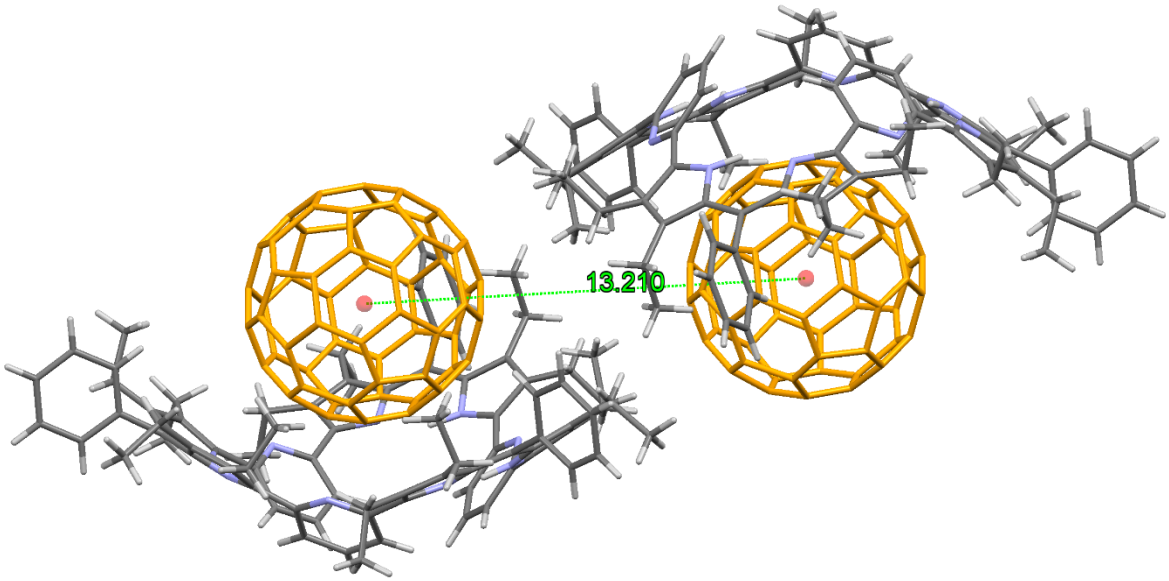

Figure S14. Distance (Å) between the centroids of C_{60} found in the repeating unit of the 1:1 $\mathbf{P_3P_6}$•C_{60} complex.

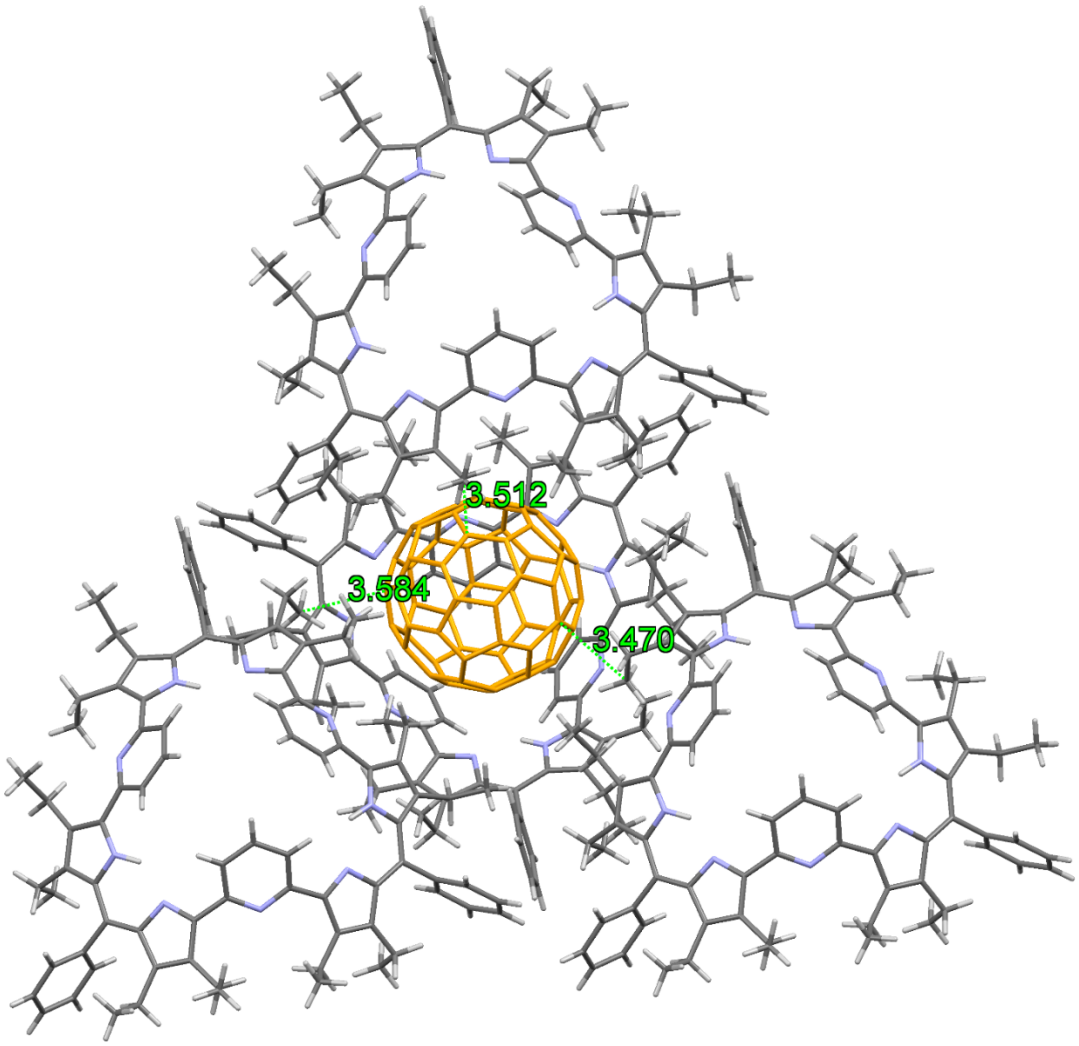

Figure S15. Interactions between C_{60} and the adjacent $\mathbf{P_3P_6}$ macrocycles as inferred from the packing diagram for the 1:1 $\mathbf{P_3P_6}$•C_{60} complex.

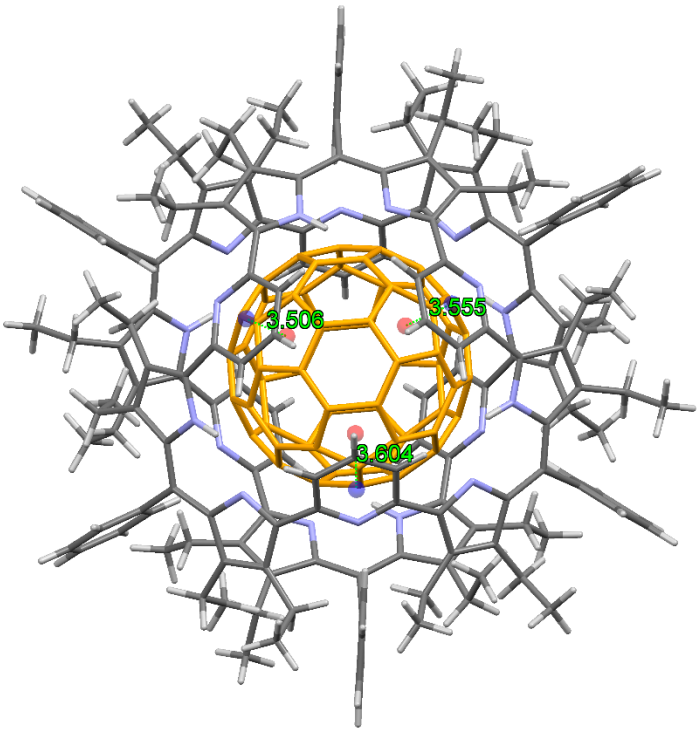

Figure S16. Distance (Å) between the center of the pyridine ring (blue balls) and the five membered rings of C_{60} (red balls) in the 2:1 $\mathbf{P_3P_6}$•C_{60} complex.

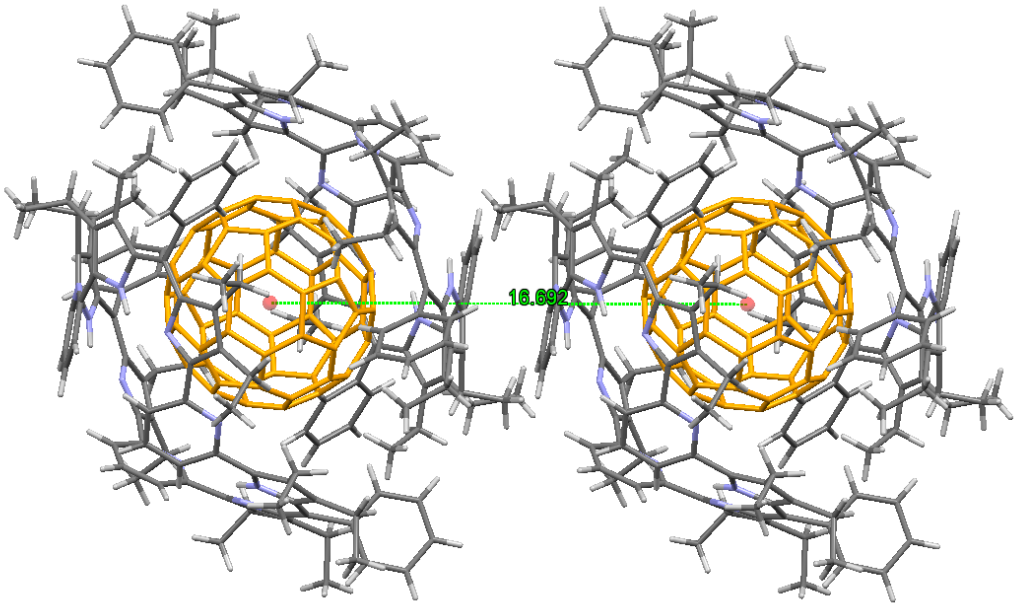

Figure S17. Distance (Å) between the center of the C_{60} guest seen in the packing of the 2:1 $\mathbf{P_3P_6}$•C_{60} complex.

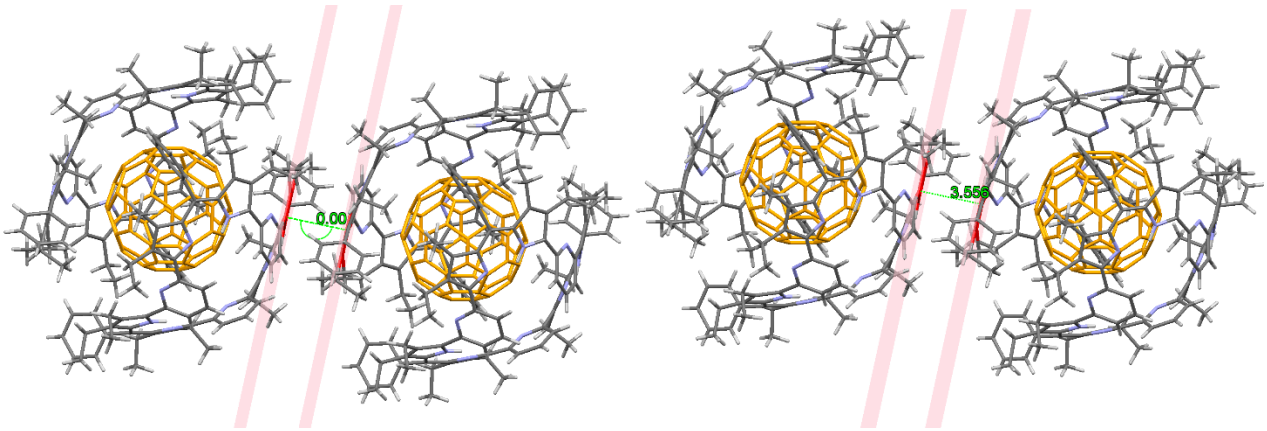

Figure S18. Pyrrole-pyrrole π-π interactions inferred from the packing arrangement seen for the 2:1 $\mathbf{P_3P_6}$•C_{60} complex.

X-ray experimental for P_3P_6 (CCDC number:1525293)

Crystals grew as thin, red needles by vapor diffusion of hexanes to a dichloromethane solution of the macrocycle. The data crystal had approximate dimensions; 0.37 x 0.04 x 0.04 mm. The data were collected on an Agilent Technologies SuperNova Dual Source diffractometer using a μ-focus Cu Kα radiation source (λ = 1.5418 Å) with collimating mirror monochromators. A total of 677 frames of data were collected using ω-scans with a scan range of 1° and a counting time of 13 seconds per frame for frames collected with a detector offset of +/- 40.8° and 50 seconds per frame with frames collected with a detector offset of +/- 106.8°. The data were collected at 100 K using an Oxford Cryostream low temperature device. Details of crystal data, data collection and structure refinement are listed in Table S1. Data collection, unit cell refinement and data reduction were performed using Agilent Technologies CrysAlisPro V 1.171.37.31.[2] The structure was solved by direct methods using SuperFlip[3] and refined by full-matrix least-squares on F^2 with anisotropic displacement parameters for the non-H atoms using SHELXL-2014/7.[4] Structure analysis was aided by use of the programs PLATON98[5] and WinGX.[6] The hydrogen atoms were calculated in ideal positions with isotropic displacement parameters set to 1.2xUeq of the attached atom (1.5xUeq for methyl hydrogen atoms). The absolute position of the hydrogen atoms could not be determined. Results using the methods of Flack[7] and the Hooft[8] were inconclusive.

The function, $\Sigma w(|F_O|^2 - |F_C|^2)^2$, was minimized, where $w = 1/[(\sigma(F_O))^2 + (0.0527*P)^2 + (0.6104*P)]$ and $P = (|F_O|^2 + 2|F_C|^2)/3$. $R_W(F^2)$ refined to 0.0884, with R(F) equal to 0.0358 and a goodness of fit, S, = 1.03. Definitions used for calculating R(F), $R_W(F^2)$ and the goodness of fit, S, are given below.[9] The data were checked for secondary extinction effects but no correction was necessary. Neutral atom scattering factors and values used to calculate the linear absorption coefficient are from the International Tables for X-ray Crystallography (1992).[10]

Table S1. Crystal data and structure refinement for P_3P_6.

Empirical formula	C84 H87 N9	
Formula weight	1222.62	
Temperature	100(2) K	
Wavelength	1.54184 Å	
Crystal system	trigonal	
Space group	R 3 c :H	
Unit cell dimensions	a = 33.1271(7) Å	a= 90°.
	b = 33.1271(7) Å	b= 90°.
	c = 10.8586(3) Å	g = 120°.
Volume	10319.8(5) $Å^3$	
Z	6	
Density (calculated)	1.180 Mg/m^3	
Absorption coefficient	0.533 mm^{-1}	
F(000)	3924	
Crystal size	0.370 x 0.040 x 0.040 mm^3	
Theta range for data collection	2.668 to 73.526°.	
Index ranges	-39<=h<=39, -39<=k<=41, -13<=l<=9	
Reflections collected	13468	
Independent reflections	4003 [R(int) = 0.0425]	
Completeness to theta = 67.684°	99.8 %	
Absorption correction	Semi-empirical from equivalents	
Max. and min. transmission	1.00 and 0.697	
Refinement method	Full-matrix least-squares on F^2	
Data / restraints / parameters	4003 / 1 / 289	
Goodness-of-fit on F^2	1.032	
Final R indices [I>2sigma(I)]	R1 = 0.0358, wR2 = 0.0849	
R indices (all data)	R1 = 0.0417, wR2 = 0.0884	
Absolute structure parameter	0.1(6)	
Extinction coefficient	n/a	
Largest diff. peak and hole	0.151 and -0.222 e.$Å^{-3}$	

X-ray experimental for P_3P_6•C_{60} 1:1 complex (CCDC number:1525294)

Crystals grew as clusters of highly intertwined, black prisms upon vapor diffusion of n-heptane into a toluene solution containing the host and guest in 1:1 host/guest mole ratio. The data crystal was cut from a large cluster of crystals and had approximate dimensions; 0.15 x 0.11 x 0.049 mm. The data were collected on an Agilent Technologies SuperNova Dual Source diffractometer using a μ-focus Cu Kα radiation source (λ = 1.5418 Å) with collimating mirror monochromators. A total of 1022 frames of data were collected using ω-scans with a scan range of 1° and a counting time of 12 seconds per frame using a detector offset of +/- 41.9° and a counting time of 30 seconds per frame using a detector offset of +/- 110.4°. The data were collected at 100 K using an Oxford Cryostream low temperature device. Details of crystal data, data collection and structure refinement are listed in Table S2. Data collection, unit cell refinement and data reduction were performed using Agilent Technologies CrysAlisPro V 1.171.37.31.[2] The structure was solved by direct methods using SHELXT[11] and refined by full-matrix least-squares on F^2 with anisotropic displacement parameters for the non-H atoms using SHELXL-2014/7.[4] Structure analysis was aided by use of the programs PLATON98[5] and WinGX.[6] The hydrogen atoms on carbon were calculated in ideal positions with isotropic displacement parameters set to 1.2xUeq of the attached atom (1.5xUeq for methyl hydrogen atoms). The hydrogen atoms bound to the pyrrole ring nitrogen atoms were observed in a ΔF map and refined with isotropic displacement parameters.

A molecule of n-heptane was found to be badly disordered around a crystallographic inversion center at ½, 1, ½. Attempts to model the disorder were unsatisfactory. The contributions to the scattering factors due to this solvent molecule were removed by use of the utility SQUEEZE[12] in PLATON98. PLATON98 was used as incorporated in WinGX.

The function, $\Sigma w(|F_o|^2 - |F_c|^2)^2$, was minimized, where $w = 1/[(\sigma(F_o))^2 + (0.1249*P)^2 + (4.0613*P)]$ and $P = (|F_o|^2 + 2|F_c|^2)/3$. $R_w(F^2)$ refined to 0.244, with R(F) equal to 0.0824 and a goodness of fit, S, = 1.04. Definitions used for calculating R(F), $R_w(F^2)$ and the goodness of fit, S, are given below.[9] The data were checked for secondary extinction effects but no correction was necessary. Neutral atom scattering factors and values used to calculate the linear absorption coefficient are from the International Tables for X-ray Crystallography (1992).[10]

Table S2. Crystal data and structure refinement for P_3P_6•C_{60} 1:1 complex.

Empirical formula	C144 H87 N9	
Formula weight	1943.22	
Temperature	100(2) K	
Wavelength	1.54184 Å	
Crystal system	triclinic	
Space group	P -1	
Unit cell dimensions	a = 16.7655(7) Å	a= 112.270(4)°.
	b = 17.4824(9) Å	b= 99.654(4)°.
	c = 20.3823(9) Å	g = 108.913(4)°.
Volume	4933.6(4) $Å^3$	
Z	2	
Density (calculated)	1.308 Mg/m^3	
Absorption coefficient	0.590 mm^{-1}	
F(000)	2028	
Crystal size	0.150 x 0.110 x 0.049 mm^3	
Theta range for data collection	2.882 to 75.601°.	
Index ranges	-20<=h<=21, -21<=k<=21, -20<=l<=25	
Reflections collected	31923	
Independent reflections	19578 [R(int) = 0.0629]	
Completeness to theta = 67.684°	99.1 %	
Absorption correction	Semi-empirical from equivalents	
Max. and min. transmission	1.00 and 0.814	
Refinement method	Full-matrix least-squares on F^2	
Data / restraints / parameters	19578 / 2 / 1434	
Goodness-of-fit on F^2	1.035	
Final R indices [I>2sigma(I)]	R1 = 0.0824, wR2 = 0.2179	
R indices (all data)	R1 = 0.1023, wR2 = 0.2437	
Extinction coefficient	n/a	
Largest diff. peak and hole	1.867 and -0.530 $e.Å^{-3}$	

X-ray Experimental for the 2:1 complex of P_3P_6 with C_{60} (CCDC number:1525295)

Crystals grew as red needles by vapor diffusion of n-heptane into toluene in 2:1 host/guest mole ratio. The data crystal was cut from a larger crystal and had approximate dimensions; 0.25 x 0.06 x 0.04 mm. The data were collected on an Agilent Technologies SuperNova Dual Source diffractometer using a μ-focus Cu Kα radiation source (λ = 1.5418 Å) with collimating mirror monochromators. A total of 1041 frames of data were collected using ω-scans with a scan range of 1° and a counting time of 25 seconds per frame with a detector offset of +/- 41.9° and 83 seconds per frame with a detector offset of +/- 111.0°. The data were collected at 100 K using an Oxford Cryostream low temperature device. Details of crystal data, data collection and structure refinement are listed in Table S3. Data collection, unit cell refinement and data reduction were performed using Agilent Technologies CrysAlisPro V 1.171.37.31.[2] The structure was solved by direct methods using SHELXT[11] and refined by full-matrix least-squares on F^2 with anisotropic displacement parameters for the non-H atoms using SHELXL-2014/7.[4] Structure analysis was aided by use of the programs PLATON98[5] and WinGX.[6] The hydrogen atoms were calculated in ideal positions with isotropic displacement parameters set to 1.2xUeq of the attached atom (1.5xUeq for methyl hydrogen atoms).

The C_{60} molecule resides around a crystallographic inversion center at ½, ½, ½. The toluene molecule is disordered around a crystallographic inversion center at 0, ½, 0. One phenyl ring and two ethyl groups were disordered. The disorder was modeled in the same way for each group. For example, for the phenyl ring, the site occupancy factor for one component of the ring was set to the variable x. The site occupancy factor for the alternate component was set to (1-x). The variable x was refined while refining a common isotropic displacement parameter for all the affected atoms. The geometry of the two rings was restrained to be equivalent throughout the refinement process.

The function, $\Sigma w(|F_o|^2 - |F_c|^2)^2$, was minimized, where $w = 1/[(\sigma(F_o))^2 + (0.0801*P)^2 + (0.5577*P)]$ and $P = (|F_o|^2 + 2|F_c|^2)/3$. $R_W(F^2)$ refined to 0.276, with R(F) equal to 0.0934 and a goodness of fit, S, = 1.20. Definitions used for calculating R(F), $R_W(F^2)$ and the goodness of fit, S, are given below.[9] The data were checked for secondary extinction effects but no correction was necessary. Neutral atom scattering factors and values used to calculate the linear absorption coefficient are from the International Tables for X-ray Crystallography (1992).[10]

Table S3. Crystal data and structure refinement for the 2:1 complex of P_3P_6 with C_{60}.

Empirical formula	C235 H182 N18	
Formula weight	3257.98	
Temperature	100(2) K	
Wavelength	1.54184 Å	
Crystal system	triclinic	
Space group	P -1	
Unit cell dimensions	a = 16.2770(10) Å	α= 108.487(7)°.
	b = 16.6922(12) Å	β= 105.496(6)°.
	c = 18.7187(13) Å	γ = 107.046(6)°.
Volume	4232.2(6) $Å^3$	
Z	1	
Density (calculated)	1.278 Mg/m^3	
Absorption coefficient	0.576 mm^{-1}	
F(000)	1718	
Crystal size	0.25 x 0.06 x 0.04 mm^3	
Theta range for data collection	3.066 to 77.449°.	
Index ranges	-18<=h<=20, -20<=k<=19, -22<=l<=14	
Reflections collected	26435	
Independent reflections	16497 [R(int) = 0.0835]	
Completeness to theta = 67.684°	97.2 %	
Absorption correction	Semi-empirical from equivalents	
Max. and min. transmission	1.00 and 0.700	
Refinement method	Full-matrix least-squares on F^2	
Data / restraints / parameters	16497 / 952 / 1285	
Goodness-of-fit on F^2	1.198	
Final R indices [I>2sigma(I)]	R1 = 0.0934, wR2 = 0.2221	
R indices (all data)	R1 = 0.1361, wR2 = 0.2763	
Extinction coefficient	n/a	
Largest diff. peak and hole	0.602 and -0.492 $e.Å^{-3}$	

6. DFT calculation details

Quantum mechanical calculations were carried out with Gaussian 09 program suite.[13] Geometry optimization in ground state (S_0) was performed by density functional theory (DFT) method with B3LYP,[14] employing a basis set consisting of 6-31G(d) for all atoms.[15] All substituents were considered during the calculation.

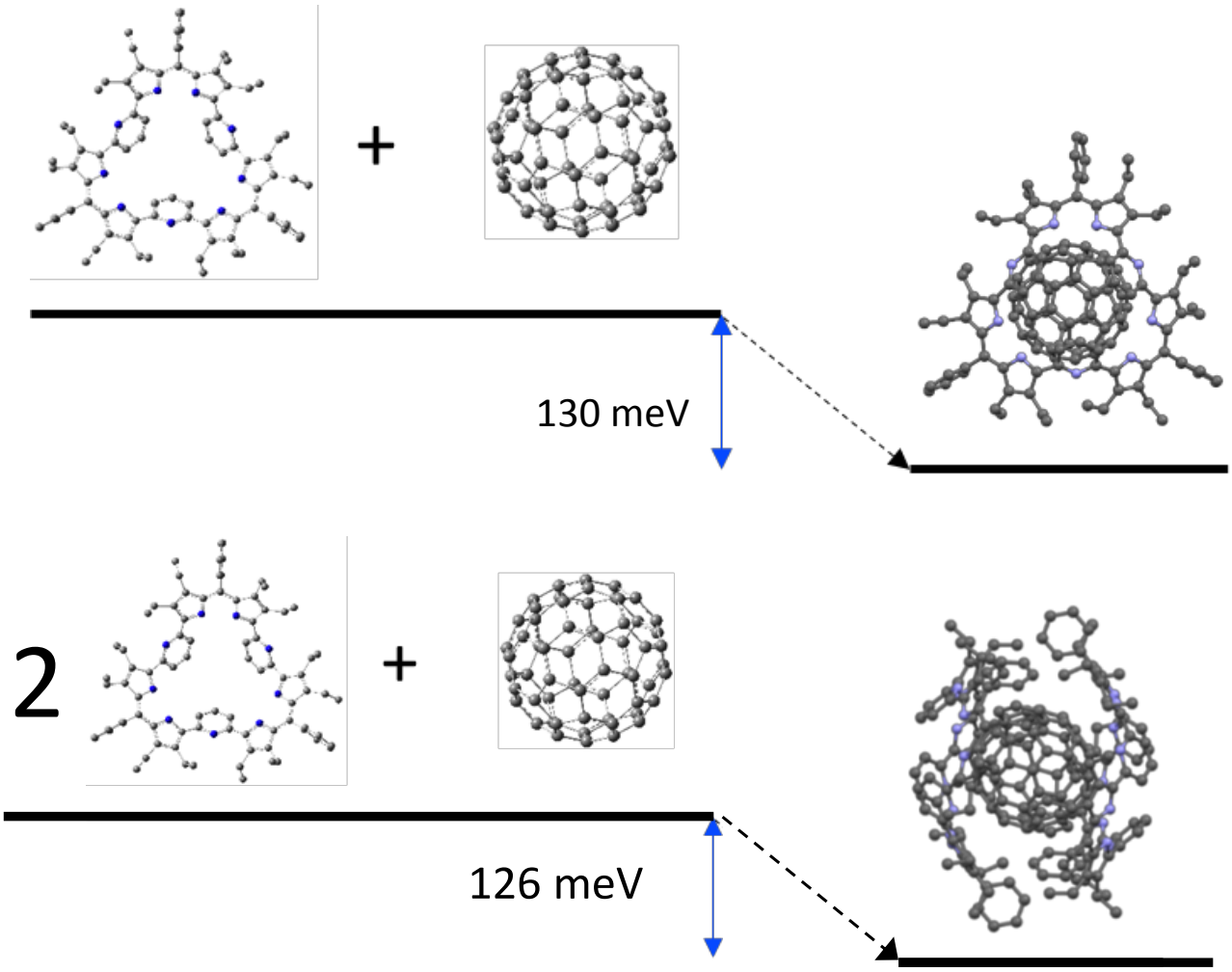

Figure S19. Optimized structure of $\mathbf{P_3P_6}$•C_{60} complexes both (top) 1:1 and (bottom) 2:1 and their binding energies compared to pristine $\mathbf{P_3P_6}$ and C_{60}.

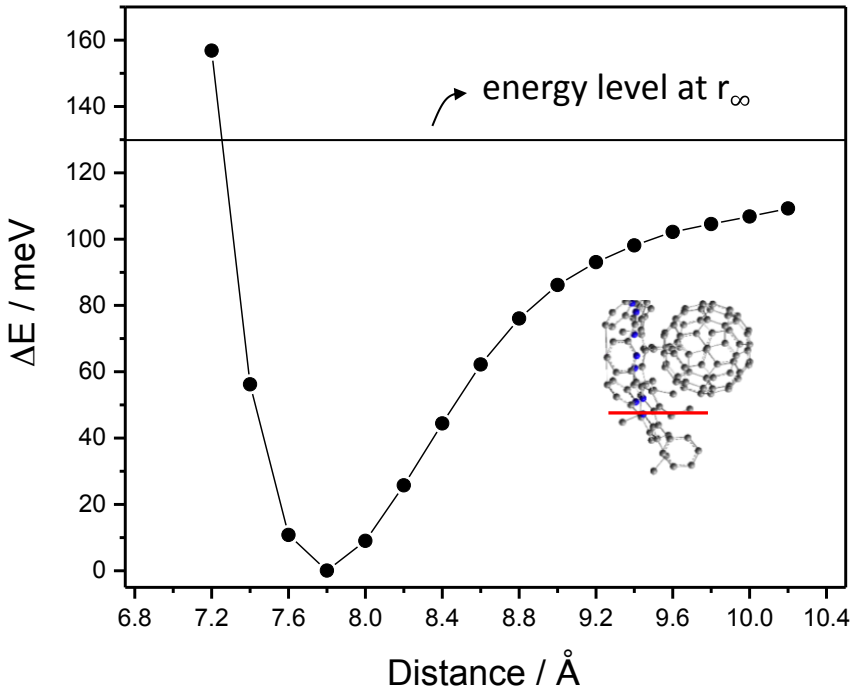

Figure S20. Relative energy of 1:1 $\mathbf{P_3P_6}$•C_{60} complex as a function of the distance between $\mathbf{P_3P_6}$ and C_{60} with a horizontal line for the energy level at r_∞.

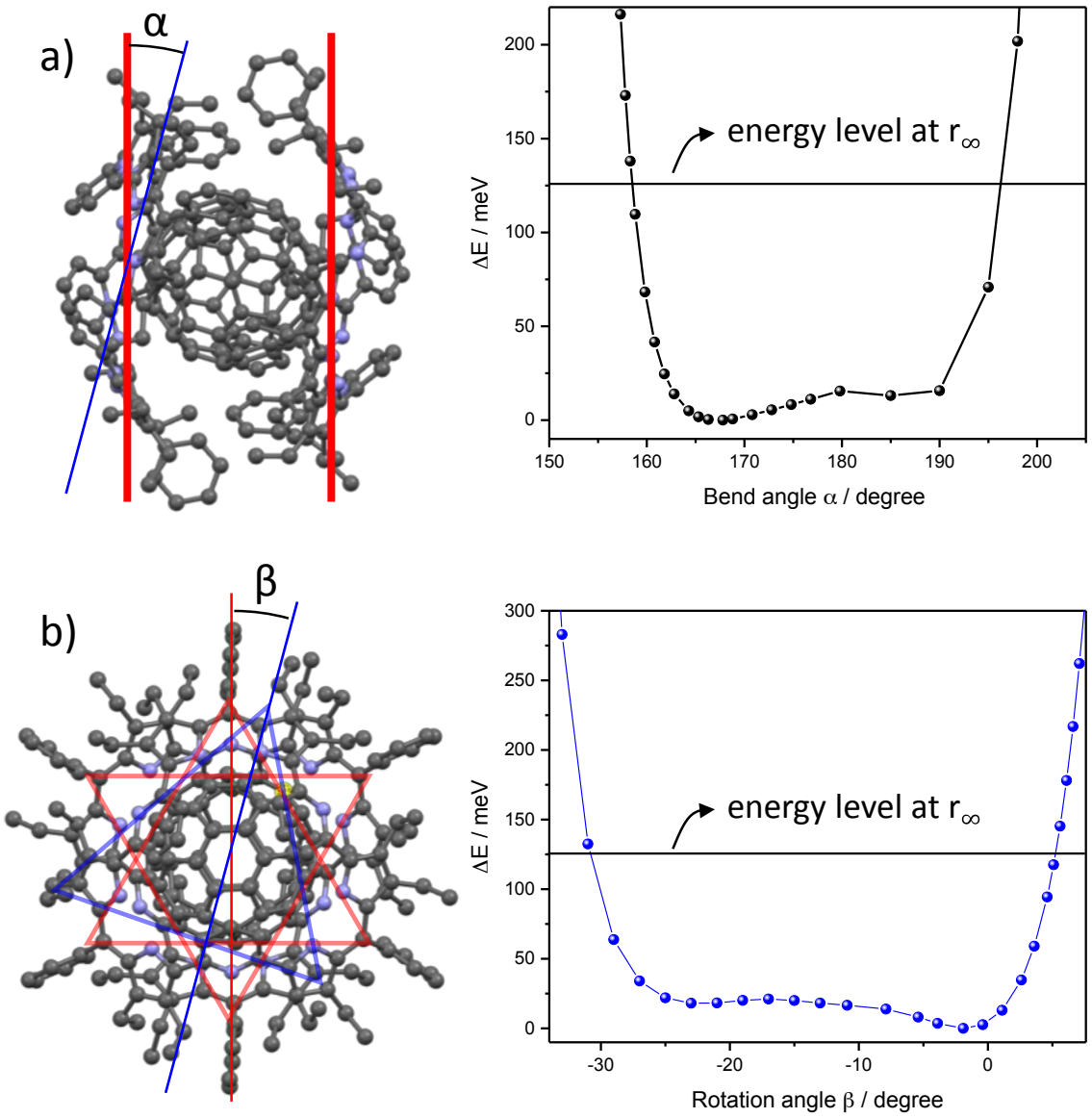

Figure S21. Relative energy of the 2:1 complex of $\mathbf{P_3P_6}$ with C_{60} as a function of (a) bend angle α where dihedral angle between two planes (zero degree for the reference two parallel red planes) and (b) rotation angle β from the reference red line with a horizontal lines for the energy level at r_∞.

7. References

1. (a) Thordarson, P. *Chem. Soc. Rev.*, 2011, *40*, 1305–1323; (b) http://www.supramolecular.org.
2. CrysAlisPro. Agilent Technologies. Agilent Technologies UK Ltd., Oxford, UK, SuperNova CCD System, CrysAlicPro Software System, 1.171.37.31, 2013.
3. Palatinus, L. and Chapuis, G. *J. Appl. Cryst.*, 2007, *40*, 786-790.
4. Sheldrick, G. M. *Acta Cryst.*, 2015, *C71*, 9-18.
5. Spek, A. L. PLATON, A Multipurpose Crystallographic Tool. Utrecht University, The Netherlands, 1998.
6. Farrugia, L. J. *J. Appl. Cryst.*, 1999, *32*, 837-838.
7. Flack, H. D. *Acta Cryst.*, 1983, *A39*, 876-881.
8. Hooft, R. W. W., Straver, L. H. and Spek, A. L. *J. Appl. Cryst.*, 2008, *41*, 96-103.
9. $R_w(F^2) = \{\Sigma w(|F_o|^2 - |F_c|^2)^2/\Sigma w(|F_o|)^4\}^{1/2}$ where w is the weight given each reflection.

   $R(F) = \Sigma(|F_o| - |F_c|)/\Sigma|F_o|\}$ for reflections with $F_o > 4(\sigma(F_o))$.

   $S = [\Sigma w(|F_o|^2 - |F_c|^2)^2/(n - p)]^{1/2}$, where n is the number of reflections and p is the number of refined parameters.
10. International Tables for X-ray Crystallography. Vol. C, Tables 4.2.6.8 and 6.1.1.4, A. J. C. Wilson, editor, Boston: Kluwer Academic Press, 1992.
11. Sheldrick, G. M. *Acta Cryst.*, 2015, *A71*, 3-8.
12. Sluis, P. v. d. and Spek, A. L. *Acta Cryst.*, 1990, *A46*, 194-201.
13. Frisch, M. J.; Trucks, G. W.; Schlegel, H. B.; Scuseria, G. E.; Robb, M. A.; Cheeseman, J. R.; Scalmani, G.; Barone, V.; Mennucci, B.; Petersson, G. A.; Nakatsuji, H.; Caricato, M.; Li, X.; Hratchian, H. P.; Izmaylov, A. F.; Bloino, J.; Zheng, G.; Sonnenberg, J. L.; Hada, M.; Ehara, M.; Toyota, K.; Fukuda, R.; Hasegawa, J.; Ishida, M.; Nakajima, T.; Honda, Y.; Kitao, O.; Nakai, H.; Vreven, T.; Montgomery, Jr., J. A.; Peralta, J. E.; Ogliaro, F.; Bearpark, M.; Heyd, J. J.; Brothers, E.; Kudin, K. N.; Staroverov, V. N.; Kobayashi, R.; Normand, J.; Raghavachari, K.; Rendell, A.; Burant, J. C.; Iyengar, S. S.; Tomasi, J.; Cossi, M.; Rega, N.; Millam, J. M.; Klene, M.; Knox, J. E.; Cross, J. B.; Bakken, V.; Adamo, C.; Jaramillo, J.; Gomperts, R.; Stratmann, R. E.; Yazyev, O.; Austin, A. J.; Cammi, R.; Pomelli, C.; Ochterski, J. W.; Martin, R. L.; Morokuma, K.; Zakrzewski, V. G.; Voth, G. A.; Salvador, P.; Dannenberg, J. J.; Dapprich, S.; Daniels, A. D.; Farkas, Ö .; Foresman, J. B.; Ortiz, J. V.; Cioslowski, J.; Fox, D. J. *Gaussian 09*, revision A.1; Gaussian Inc.; Wallingford CT, 2009.
14. Yanai, T., Tew, D. P. and Handy, N. C. *Chem. Phys. Lett*. 2004, *393*, 51-57.
15. Ditchfield, R., Hehre, W. J. and Pople, J. A. *J. Chem. Phys*. 1971, *54*, 724-728.